Limnology

Effects of winter flooding on phosphorus dynamics in rice fields

--Manuscript Draft--

Manuscript Number:	LIMN-D-19-00110R5
Full Title:	Effects of winter flooding on phosphorus dynamics in rice fields
Article Type:	S.I. : Phosphorus cycle in watersheds (Part1)
Corresponding Author:	Takuya Ishida Research Institute for Humanity and Nature Kyoto, Kyôto JAPAN
Corresponding Author Secondary Information:	
Corresponding Author's Institution:	Research Institute for Humanity and Nature
Corresponding Author's Secondary Institution:	
First Author:	Takuya Ishida
First Author Secondary Information:	
Order of Authors:	Takuya Ishida
	Yoshitoshi Uehara
	Tohru Ikeya
	Takashi F. Haraguchi
	Satoshi Asano
	Yohei Ogino
	Noboru Okuda
Order of Authors Secondary Information:	
Funding Information:	RHIN Project (D06-14200119) — Dr. Noboru Okuda Japan Society for the Promotion of Science (JP19K15723) — Dr. Takuya Ishida
Abstract:	Controlling phosphorous (P) loads from rice fields is important for the conservation of aquatic ecosystems, in part because P is relatively concentrated at its sources. Recently, winter flooding, by which irrigation water is maintained in rice fields during winter, has attracted much attention as a farming strategy for environmental conservation and biodiversity maintenance. However, the effects of winter flooding on nutrient cycles have received little research attention. We evaluated the effects of winter flooding on P loads in rice fields by performing laboratory experiments with soils from rice fields with/without winter flooding. These incubation experiments showed that total and soluble reactive P concentrations in surface solutions are decreased by winter flooding. This decrease may follow co-precipitation of P with iron, which may be dissolved from winter flooded soil and rapidly precipitates in solution. Periphyton, which may increase during winter flooding, may not contribute to this decrease because puddling resets periphyton quantities on surface soils. P loads from rice fields with winter flooding over 16 days after fertilization could be reduced by an average of 26% compared with those without winter flooding, indicating that winter flooding is a valuable strategy for reducing P loads in spring, when high P loads occur.
Response to Reviewers:	Thank you very much for handling and giving valuable comments to our manuscript. We have revised captions of table 1 and table S1 in supporting information. Also, captions of tables and figures have been put just above each table and figure. We have revised figures and summarized them in a word file. We hope the figure quality is sufficient for publication.

Title:

Effects of winter flooding on phosphorus dynamics in rice fields

Author:

Takuya Ishida,*[,1,2] Yoshitoshi Uehara,[1] Tohru Ikeya,[1] Takashi F. Haraguchi,[1] Satoshi Asano,[3] Yohei Ogino,[1] Noboru Okuda[1]

Affiliations:

[1]Research Institute for Humanity and Nature, 457-4, Motoyama, Kamigamo, Kyoto, 603-8047, Japan

[2]Graduate School of Adcanced Science and Engineering, Hiroshima University, 1-3-2, Kagamiyama, Higashi-Hiroshima, Hiroshima, 739-8511, Japan

[3]Graduate School of Global Environmental Studies, Kyoto University, Yoshidahonmachi, Sakyo, Kyoto, 606-8501, Japan

Abstract

Controlling phosphorous (P) loads from rice fields is important for the conservation of aquatic ecosystems, in part because P is relatively concentrated at its sources. Recently, winter flooding, by which irrigation water is maintained in rice fields during winter, has attracted much attention as a farming strategy for environmental conservation and biodiversity maintenance. However, the effects of winter flooding on nutrient cycles have received little research attention. We evaluated the effects of winter flooding on P loads in rice fields by performing laboratory experiments with soils from rice fields with/without winter flooding. These incubation experiments showed that total and soluble reactive P concentrations in surface solutions are decreased by winter flooding. This decrease may follow co-precipitation of P with iron, which may be dissolved from winter flooded soil and rapidly precipitates in solution. Periphyton, which may increase during winter flooding, may not contribute to this decrease because puddling resets periphyton quantities on surface soils. P loads from rice fields with winter flooding over 16 days after fertilization could be reduced by an average of 26% compared with those without winter flooding, indicating that winter flooding is a valuable strategy for reducing P loads in spring, when high P loads occur.

Keywords:

phosphorus load; redox condition; iron dynamics; incubation experiment; rice field soil

1. Introduction

Because phosphorus (P) is an essential element for all living organisms and can be a limiting factor for primary production in aquatic ecosystems, anthropogenic P loads in aquatic ecosystems have caused serious water pollution and eutrophication. In developed countries, watershed management has been practiced using institutional and technological approaches to reduce P loads from point sources and mitigate eutrophication (Carpenter et al. 1998; Kagatsume 2012). In contrast, controlling P loads from non-point sources, such as agricultural and urban activities, is increasingly important because these sources are increasingly predominant relative to point sources (Sharpley 2016). Agricultural land is one of the most important sources of P due to the use of fertilizers (Kim et al. 2018; Carpenter et al. 1998; Sharpley 2016; Ishida et al. 2019). However, agricultural inputs of nutrients are difficult to regulate because they are derived from activities over wide areas (Carpenter et al. 1998) and include many stakeholders such as farmers, governments, and private sectors. The involvement of multiple stakeholders creates difficulties regarding reaching a consensus about reduction of P load because of conflicts among them.

Rice fields are dominant among agricultural areas in monsoonal Asia. In Japan, rice fields occupied 54.4% of agricultural land in 2018 (MIC 2018). Generally, paddy irrigation and puddling and rice planting are performed in spring in Japan. Nutrients from fertilizers often pollute water downstream due to puddling and water discharge from rice fields (Hua et al. 2017; Okubo et al. 2014; Sharpley et al. 2007; Yamada et al. 2006). Therefore, it is important to control P loads during spring.

Recently, winter flooding, in which irrigation water is maintained in rice fields during winter, has attracted much attention as an environmentally conservative farming strategy throughout Japan and East Asia (Takada et al. 2014). Winter flooding provides wetland habitats for aquatic organisms, such as frogs, salamanders, small fish, and migratory birds during winter (Asano et al. 2018; Makiyama and Tsukamoto 2006; Somura et al. 2015). In addition, biogeochemical studies on the effects of winter flooding have been conducted to describe carbon and nitrogen cycles in flooded rice fields. These cycles are related to the emission of greenhouse gases including methane and nitrous oxide (Fitzgerald et al. 2000; Kudo et al. 2017; Zhou et al. 2017). Furthermore, winter flooding may affect P cycles by changing soil physicochemistry and the activities of organisms. However, the understanding about how winter flooding affects P dynamics in rice fields is poor because only a few studies on this topic have been performed (Somura et al. 2015).

A potential effect of winter flooding on P cycles involves the progression of reductive conditions in soils. Labile P pools in soils are generally small because P is strongly adsorbed to or bound to iron (Fe), aluminum (Al), and calcium (Ca) (Reddy et al. 1999). Reductive soil conditions change P dynamics by reducing Fe^{3+} to Fe^{2+}, which results in the dissolution of Fe-bound phosphate, thus increasing P concentrations in irrigation water. In contrast, the dissolution of Fe^{2+} may reduce P concentrations in irrigation water by causing rapid Fe^{2+} oxidation and co-precipitation with dissolved P (Li et al. 2017).

Increases in periphyton during winter flooding may also affect P cycles in rice fields. Periphyton is an ubiquitous autotroph in flooded rice fields and affects P dynamics through biotic and abiotic processes (Li et al. 2017). As a biotic process, taking P by periphyton from soil, sediment, and water directly affects P cycles (Reddy et al. 1999). In addition, periphyton proliferates after irrigation and changes local chemical environments by photosynthesizing and respiring (Scinto and Reddy 2003). Periphyton photosynthesis increases pH in surrounding water during the day, which promotes Ca-phosphate precipitation and deposition of carbonate–phosphate complexes (Woodruff et al. 1999). Moreover, periphyton can produce super-saturated O_2 concentrations near the soil surface through photosynthesis, further encouraging deposition of Fe- and Al-bound P by maintaining oxidizing conditions in soil and water columns (Dodds 2003). Therefore, chemical and biological processes that are related to winter flooding alter P dynamics by changing the conditions in rice fields prior to farming operations, such as puddling soil, adding fertilizer, and planting rice, and thus contribute to decreases or increases in P efflux from rice fields.

To evaluate the effects of winter flooding on P dynamics, we incubated soil samples from rice fields following winter flooding and compared them with samples from conventional fields in which no winter flooding had been performed. In rice fields, natural and human factors are tightly linked, hampering efforts to distinguish the effects of winter flooding. In the present experiment, we were able to control these factors, especially human factors, allowing the accurate evaluation of the effects of winter flooding. Because the efflux of P loads from rice fields into aquatic ecosystems is the highest after fertilization (Hua et al. 2017; Okubo et al., 2014; Sharpley et al., 2007; Yamada et al. 2006), P concentrations in incubated samples were monitored for 27 days after fertilization. To investigate factors that affect P dynamics, we also determined dissolved metal concentrations, oxidation–reduction potentials (ORP), P concentrations, and chlorophyll *a* (chl *a*) concentrations in soil and water samples.

2. Methods

2.1. Study site

The present study was conducted in the Kosaji area, which is a mesomountainous region in Shiga prefecture, central Japan (34°945′–34°921′N, 136°200′–136°241′E; Fig. 1). The experimental rice fields were located in a gully with the geology of a Paleo-lake Biwa layer, which was formed about 2.5 million years ago. The soil from this layer is rich in clay and is classified as Typic Hydraquent according to soil taxonomy (Soil Survey Staff 2010). Irrigation water for the paddies in the study area comes from ponds in the Kosaji area and is piped from an agricultural dam in the upper area of Kosaji. The ponds are available as a water source throughout the year, but the dam is only used for irrigation during the growing season from April to October.

Farmers in Kosaji have conducted winter flooding as an environmental conservation activity since 2015. The clay soils of Kosaji help to keep irrigation water in the rice fields without the need for frequent additions of water. To support winter flooding as environmental conservation activity, Shiga Prefecture subsidizes farmers who participate in the activity.

2.2. Sample collection

Five sampling plots (site IDs were K1–K5) were selected for incubation experiments (Table 1 and Fig. 1). Each plot included paired winter flooded rice fields

(WF) and conventional rice fields without winter flooding (CT). Paired rice fields for K3 and K4 were operated by same farmers, respectively. Thus, the history of farming practice (e.g., type and amount of fertilizers and water management) was similar between WF and CT for K3 and K4. The history of other plots might be different because they are owned by different farmers. However, the farmers followed the instruction of Japan Agricultural Cooperation; therefore, there are no huge differences in farming practices between WF and CT for all plots, except for winter flooding. The WF had been flooded for more than 2 months before sample collection (Table 1), which was conducted on April 3, 2017. The sampling depth was 0–20 cm, which corresponds with the cultivated layer. Due to the spatial heterogeneity of these soils, five samples were collected from every rice field and were mixed well using a shovel to obtain averaged chemical properties for incubation experiments. Irrigation water samples were collected from irrigation channels at each site and were combined for incubation experiments.

2.3. Incubation experiments

Subsamples were obtained from mixed soils for chemical and chl *a* analyses, which were performed to determine baseline conditions of the soil. Subsamples were sieved through 2-mm mesh, were divided into two and were stored at −30°C for chl *a* analysis or were dried at 50°C and then stored at room temperature for chemical analyses.

The remaining non-sieved soil samples were used in incubation experiments. Two-L aliquots of irrigation water were added to the soils and were mixed using a shovel to model puddling of rice fields. About 500-g mixed soil samples were then placed in five plastic tubes of 4.8 cm in diameter and 30 cm in height (five replicates for each sample). After removing aliquots of mixed water, 80-ml aliquots of irrigation water were added to maintain the same volume of water in each tube, and were mixed with the soil at a depth of 5 cm to model after puddling. Immediately after mixing, 5-ml supernatants were collected for chemical analysis as incubation day-0 samples, which corresponded to after puddling before fertilization.

To emulate fertilizer operations, chemical (magnesium multi-phosphate, Onoda Chemical Industry Co. Ltd) and organic fertilizers (Asahi Industries Co., Ltd) were ground from granulation to powder using a multi-bead shocker (Yasui Kikai, Japan) with tungsten carbide beads to homogenize and to weigh their small amount. Thereafter, 40 mg of chemicals and organic fertilizers were added to incubation tubes and were mixed with surface soil from about the top 5 cm in depth. Fertilizer types and amounts were the same as those used by farmers in Kosaji. The chemical and organic fertilizers contain 9.1% and 2.0% of P, respectively, due to guaranteed analysis by the makers. Theoretical initial total phosphorus (TP) concentration after adding the fertilizers are 55.5 mgP L^{-1}, which is calculated by fertilizer amounts and concentrations and water volume in the incubation tubes (Table 2).

Sidewalls of the incubation tubes corresponding with the soil part were wrapped in aluminum sheet to avoid exposure to light. The tubes were incubated in a room with a 13-h light/11-h dark cycle. The air temperature was set to 15°C to represent average temperatures in Kosaji during April and May. Samples were incubated for 27 days. During incubation, 50-ml aliquots of ultra-pure water were added once weekly to compensate for evaporation and 5-ml supernatants were collected on days 1, 3, 7, and 16. Immediately after water sampling, ORP in surface soils from about 1 cm in depth were measured using an ORP electrode (9300-10D with D-74, Horiba, Japan). On day 27 of incubation, all supernatant water was sampled. Water and soil samples were stored at −30°C until analysis.

2.4. Chemical analyses

We analyzed concentrations of TP, total dissolved phosphorus (TDP), and soluble reactive phosphorus (SRP) in incubated water samples. Unfiltered samples were used in determinations of TP and filtered samples through 0.2-μm membrane filters (DISMIC, 13HP020AN, Advantec, Toyo Roshi Kaisha LTD., Japan) were used for TDP and SRP analyses. Samples for TP and TDP analyses were oxidized by adding potassium peroxodisulfate and were then digested in an autoclave (JIS 1993). Thereafter, P concentrations of each fraction (TP, TDP, and SRP) were measured using the molybdenum-blue method (Murphy and Riley 1962) on a microplate spectrophotometer (Multiskan GO, Thermo Fisher Scientific, USA). We calculated concentrations of particle phosphorus (PP) and soluble nonreactive phosphorus (NRP) using the following equations:

$$\mathrm{PP} = \mathrm{TP} - \mathrm{TDP}$$

$$\mathrm{NRP} = \mathrm{TDP} - \mathrm{SRP}$$

SRP fraction, which includes orthophosphate and other labile organic and inorganic P (Tarapchak and Rubitschun 1981; Yi et al. 2019), is considered to be readily bioavailable (Reynolds and Davies 2001). In contrast, TP, PP, and NRP fractions, which include various P fractions, are considered to be less bioavailable than SRP (Reynolds and Davies 2001).

Dissolved Al, Fe, and Ca concentrations in filtered water samples were determined using inductively coupled plasma-optical emission spectroscopy (ICP-OES; iCAP 6200, Thermo Fisher Scientific, USA). We analyzed water chemistry from three replicates that were in average incubation state.

Soil samples were used for analyses of initial physicochemical properties prior to incubation (initial subsample). In these analyses, soil pH was determined using a glass electrode (9625-10D with D-74, Horiba, Japan) in a 2.5:1 deionized water/soil suspension. Concentrations of organic matter were measured as ash-free dry mass in soil samples after combustion at 500°C. Soil texture was determined using a laser diffraction particle size analyzer (SALD-2200, Shimadzu, Japan) after decomposition of organic matter with 30% H_2O_2 solution and ultrasonic dispersion of soil particles in 1-M HCl solution, as described previously (Day, 1965). To determine P concentrations in each fraction, we performed sequential extraction according to Hupfer et al. (1995). Briefly, soil samples were sequentially extracted using 1-M NH_4Cl, 0.11-M $NaHCO_3/Na_2S_2O_4$ (BD), 1-M NaOH, and then 1-M HCl solutions. P fractions of each extract solution included loosely absorbed P (NH_4Cl-P), reductant soluble P (BD-P), metal oxide bound P (NaOH-P), and calcium bound P (HCl-P). Extract solutions were filtered through 0.2-µm membrane filters and SRP and NRP were then measured as described above. We also analyzed the same chemical properties after incubating soil samples that were taken at depths of 0–5, 5–10, and 10–20 cm from sites K4 and K5. P concentrations in incubated water samples were observed in two patterns, as described in the results and discussions sections. K4 and K5 sites were representative of each pattern.

To determine chl *a* contents in soil, samples were analyzed before and after incubation. Soil samples after incubation were analyzed at a depth of 0–1 cm and chl *a* concentrations were determined by extracting with dimethylformamide (Suzuki and Ishimaru 1990) and analyzing extracts with a fluorescence spectrometer (F-4500, Hitachi High-Technologies, Japan). The chl *a* after incubation were measured in triplicates from a soil sample collected from an incubation tube.

2.5. Statistical analysis

We did not apply a substrate-dependent process model but applied a regression-based model, because P reduction in the incubation water is caused by a complex of mechanisms with different kinetics, such as adsorption on soil minerals and biological uptake. Because we sampled soil using a split-plots design and made repeated measurements of water in each incubation tube, we applied linear mixed-effect regression (LMM) to select best-fit models and to estimate parameters for analyzing decay of TP concentration in incubation water. Model selections were based on Akaike information criterion (AIC). In post-hoc tests, the variable of interest had more than two levels and Tukey all-pair comparisons were conducted to adjust *p* values. All statistical analyses were conducted using R version 3.5.1 (R Core Team 2018). Packages “lme4” and “multcomp” were used for the LMM model fitting and for post-hoc tests.

To analyze decay of TP concentrations in water over the course of incubation (day), TP data from days 1–27 were used. TP concentrations were log-transformed and normalized, and the same statistical procedure was applied to TP on day 0.

To consider unknown effects of incubation on TP, incubation tube IDs, which were assigned to each replication, were set as a random intercept and variations of TP decay over the incubation period were considered by applying a numerical incubation-duration variable as a random slope. We then evaluated the effects of winter flooding practices and sampling sites on the decay of TP in water in two steps. We intended to show how these factors interact with each other. In the first step, we used all TP data from days 1 to 27 with factorial variables of water flooding practices and site IDs (K1–K5). Numerical variables of incubation-duration and all interaction terms were applied as fixed variables for the full model explaining TP in water. In the second step, LMM with water flooding practices, incubation-durations, and interaction terms between them, were included as fixed explanatory variables and were applied to each of the TP data-subsets, which were separated by soil-sampling site.

The full model for TP in water was also used to estimate the decay rates of TP in water samples from all sampling sites and flooding practice types. Before estimating decay rates using TP data from all incubation results, incubation-durations were transformed to a factorial variable and were applied with post-hoc tests to decide whether decay rates should be calculated using measurements from days 1–27. We estimated TP from fertilizers in water until the day after comparisons showed no significant differences and TP data were cut off for calculating the decay rate.

The effects of water flooding practices, site IDs, and interactions between these variables on changes in ORP throughout the incubation period were evaluated to investigate the progress of redox reactions over the incubation period. Due to small sample sizes for ORP measurements, LMM with site ID as a random intercept and day as a random slope caused false convergence. Thus, in a simpler linear model (LM), flooding practice, site ID, day, and interaction terms were applied as fixed variables in the regression model of ORP measurements. To identify sites at which water flooding practices affected ORP, best-fit LMs explaining ORP data during incubation were selected for each sampling site. Similar to other model selections, evaluations of model fit were conducted using AIC.

3. Results

The present incubation experiments indicated two differing patterns of P dynamics in samples. Therefore, we took the average value from all sites, and assigned K4 and K5 as representative of each pattern. Results from the other sites are shown in the supplementary information.

3.1. Chemical and physical properties of soils before and after incubation

Initial soil chemistry is shown in Table 1. Soil pH ranged from 5.7 to 6.3 and there were no differences between WF and CT. Organic matter concentrations in K1 were higher for WF than for CT. In contrast, organic matter concentrations of K3 and K5 were lower for WF than for CT. Concentrations of each P fraction in soils were generally lower for WF than for CT except for those in K1. Soil texture was classified as loam in K4 and silty clay loam in the other four sites, according to the criteria of the International Society of Soil Science. After incubation, soil chemistry differed little from that in initial samples (see Table S1).

3.2. P, Al, Fe, and Ca concentrations in incubated water

Before fertilizers were added (day 0), TP concentrations in incubated water were lower for WF than for CT, except at site K2 (Fig. 2). Flooding practices were selected in the model, and explained TP contents in water on day 0 (model AIC = 101, null AIC = 136, model degrees of freedom (DF) = 4). According to this model, TP concentrations were lower for WF (0.30 mgL^{-1}) than for CT (1.00 mgL^{-1}; see Table S2). The dominant P fraction in TP was PP, which was also present at lower concentrations in WF sites than in CT sites.

After adding fertilizer, TP in incubated water immediately increased to near theoretical initial TP concentration (55.5 mg L^{-1}) and then gradually decreased by day 16 at all sites (Figs. 3 and S1). TP concentrations of K1 and K4 were lower for WF than for CT. SRP was the dominant fraction of TP and showed a similar trend to TP (Figs. 4 and S2). The highest PP concentrations were observed during days 1–7 (see Fig. S3). Although PP concentrations at sites K1 and K2 increased from days 16 to 27, this increase may reflect soil particle contamination during sample collection on day 27 (see material and method). NRP concentrations were undetectable except on day 1 (see Fig. S4).

The following fixed variables were selected in a best-fit model for explaining TP concentrations in incubated water after addition of fertilizer: incubation-duration, site ID, water flooding practice, and interactions between site IDs and water flooding practices (model AIC = 408, null AIC = 424, model DF = 15; see Table S3). Even when incubation times (days) were transformed as a factor variable, they were consistently selected (model AIC = 325, null AIC = 503, model DF = 9; see Table S3). Post-hoc multiple comparisons of TP concentrations between samples with differing incubation-durations revealed that TP values were significantly different between days 1 and 16 ($|z| > 3.8$, $p < 0.005$; see Table S4), yet differences in TP contents did not differ significantly between days 16 and 27 ($|z| = 1.5$, $p = 0.55$; see Table S4). These results indicate that water TP from added fertilizer is processed by 16 days after incubation, and in some sampling sites this TP process was affected by winter flooding practices.

Best-fit LMMs explaining TP data-subsets, which were separated by soil-sampling sites, confirmed that TP decreased during incubation irrespective of sampling site, and decay rates did not show clear differences between WF and CT. For example, no interaction term between flooding practice and incubation-duration was selected (Table 3). In the best-fit models for data-subsets from sites K1 and K4, flooding practices were selected as another fixed variable. In the ensuing analyses, AIC improved by 2.4 for site K1 data and by 7.7 for site K4 data. In contrast, in data-subsets from other sites, this variable was not selected but increased AIC by at least 1.8. Based on model-estimated decay rates, log-transformed TP decreased with incubation days 1–16 at rates ranging from −0.296 to −0.126. These slopes corresponded with changes in the half-life of TP in water from 2.3 to 5.5 days (see Table S5).

Al and Fe concentrations in water were present at low values during incubation (see Figs. S5 and S6). Although Ca concentrations were high during the early stages of incubation, differences between WF and CT were not clear (see Fig. S7).

3.3. ORP values in incubated soils

ORP values in surface soils gradually decreased with incubation times (Figs. 5 and S8), with regression coefficients ranging from −7.54 to −3.93 mV day^{-1}, and variations were associated with differences between sampling sites. Flooding practice, incubation-duration, site, and interactions between flooding practice and site ID, were selected as best-fit LM to explain all ORP data during incubation (model AIC = 518, null AIC = 629, model DF = 12; see Table S6). These results indicated that decay rate of ORP (mV day^{-1}) was similar across all study sites and water flooding practice decreased soil ORP. Moreover, the interaction term between water flooding practice and site ID suggested that the effect of water flooding practice was not uniform throughout the sampling sites. In best-fit LMs for soil ORP data-subsets, which were separated and analyzed for each soil-sampling site, flooding practice was selected in all data-subsets except for that from site K5 (see Table S7). However, the ORP of the K1 data-subset and the K4 data-subset were clearly lower for WF than for CT (280 mV lower in K1, 268 mV lower in K4, based on LM estimation). Although ORP values for K2 subsets also showed similar trends as observed for K1 and K4 subsets, differences between flooding practices were not large compared with those of the former two sites. ORP values of K3- and K5-data differed little between WF and CT (differences of −15 and 37 mV, respectively).

3.4. Chl *a* concentrations in soils before and after incubation

Before incubation, chl *a* concentrations in surface soils were relatively constrained to a narrow range (Figs. 6 and S9). After incubation, chl *a* concentrations increased, but no clear trend was indicated between flooding practices for each site.

4. Discussion

4.1. Effects of winter flooding on chemical processes that influence P concentrations in irrigation water

Our incubation experiments with rice field soils indicate that winter flooding changes P dynamics in rice field ecosystems (Figs. 3–4 and S1–2), and that these changes are likely driven by chemical and biological processes.

We hypothesized that winter flooding could increase and decrease P concentrations due to chemical processes, especially the dissolution of Fe. Our determinations of TP concentrations in incubation experiments and model selection analyses showed decreases in P concentrations at sites K1 and K4 following winter flooding (Table 3 and Fig. 3 and S1). Regarding chemical processes, redox conditions in soils can promote Fe precipitation from soil, offering a possible mechanism by which changes in P dynamics are mediated. During incubation, P concentrations, especially SRP concentrations in incubated water from K1 and K4 sites, were lower for WF than for CT (Fig. 4 and S2). In addition, the ORP values of both sites were lower for WF than for CT (see Table S7 and Fig. 5 and S8). Under strong reducing conditions, the ORP value was

<100 mV at pH 7, indicating that Fe in soil was in the soluble Fe^{2+} form (Kögel-Knabner et al. 2010). Therefore, dissolved Fe^{2+} should be released from surface soils of WF at K1 and K4; in these fields, ORP values were <100 mV, relative to the ORP of incubated water during mixing of soil and addition of fertilizer. However, Fe concentrations in the incubated water from WF at K1 and K4 were not detected by the ICP-OES measurement on day 1 (see Fig. S6), indicating that dissolved Fe^{2+} from the soil was rapidly oxidized to Fe^{3+} and precipitated. Li et al. (2017) conducted kinetic experiments to evaluate the effects of Fe on the removal of dissolved P in solutions. After adding Fe^{2+}, Fe and P concentrations rapidly decreased within 1 h, suggesting that Fe^{2+} was oxidized and precipitated as $FePO_4$, vivianite, and $Fe_7(PO_4)_6$ (Huang et al. 2015; Mao et al. 2016) or P was adsorbed by ferric hydroxides. Regarding the results of the present study, P removal due to Fe oxidation explains our observations at sites K1 and K4, where differences in SRP concentrations reflected flooding practices.

As described above, redox conditions in soil may be key to decreases in P concentrations after fertilization. Winter flooding for more than 2 months (Table 1) introduced lower ORP values at sites K1 and K4 compared with those for CT (Figs. 5 and S8). However, no clear differences between the flooding practices were observed at the other sites. Redox conditions in soil after flooding are mainly controlled by microbial activities (Munch et al., 1978). Therefore, soil biology and dissolved organic matter, which affects soil biology, may differ between the present study sites. In addition, water depths of irrigation water in winter flooded rice fields varied between farmers and may also affect redox conditions in soil.

Before addition of fertilizer, TP and PP concentrations in water columns were lower for WF than for CT samples. P concentrations in initial soil samples generally had the same trend (Table 1), indicating that soil P moved from surface layers to deeper layers with the downward movement of flood water. Alternatively, P may change to a more stable fraction (residual P) during winter flooding. The sum of P fractions in the present soil samples was significantly correlated with TP concentrations in incubated water on day 0 (Pearson's $r = 0.45$; $p < 0.05$). Because PP was the dominant fraction of TP on day 0, decreased P concentrations in soil particles following winter flooding may have lowered TP concentrations in incubated water from WF sites on day 0.

4.2. Biological process effects of winter flooding on P concentrations in irrigation water

We hypothesized that volumes of periphyton on soils increase due to winter flooding and that these affect P dynamics by consuming P. However, chl *a* concentrations in initial soil samples was not affected by flooding practices (Figs. 6 and S9), potentially reflecting puddling operations before incubation. Thus, we collected soil samples to a depth of 0–20 cm at each sampling plot and mixed them. Because periphyton occurs only on surface soil, increases during winter would be obscured in our soil samples after puddling operations. Inubushi et al. (1982) reported similar results showing that chl *a* concentrations in rice field soils are highest on the surface (0–1 cm) and that puddling homogenizes chl *a* concentrations from the surface to deeper soils. Hence, the effects of winter flooding on periphyton may be abolished by puddling operations.

Although periphyton could not explain differences in P concentrations between WF and CT at K1 and K4 on day 1 (Figs. 6 and S9), P uptake and photosynthesis by periphyton may contribute to P removal from solutions throughout the incubation period regardless of the sites and flooding practices, because periphyton increased after 27 days incubation. It is reported that rates of the P uptake by periphyton reportedly range from 0.14 to 43100 mgP m^{-2} day^{-1} (Dodds 2003), which is sufficient to decrease SRP concentrations in incubated water. Photosynthesis by periphyton also promotes Fe oxidation and P removal by generating O_2 and changing redox conditions. In addition, periphyton may affect redox condition in soil during winter flooding (before sample collection) by producing labile organic matter and changing soil biology, which may contribute in the reduction of the P concentration after fertilization.

4.3. Implications of winter flooding for the management of rice fields

To estimate decreases in P loads following winter flooding, we calculated reduction ratios of TP with reference to conventional farming (WF/CT) by integrating TP concentrations over 16 days. TP concentrations on day 27 were excluded from the calculation because of particle disturbance at the sample collection site (see 3.2.2). WF/CT values for each site ranged from 0.27 to 1.08 (average 0.74), indicating that winter flooding reduces P loads from rice fields through agricultural wastewater, by up to 73% for 16 days after addition of fertilizer. To confirm this estimation is valid, field investigation is necessary. Especially, fertilizer operation in our study (fertilizers were ground to powder) may cause higher TP concentration in incubation water (Figs. 3 and S1) than that in surface water in Japanese rice fields, in which TP concentration is <26.5 mgP L^{-1} (Takamura et al. 1976; Udo et al. 2000; Okubo et al., 2014), resulting in overestimation of reduction rate by winter flooding. In addition, to conclude the effect of winter flooding on P runoff from rice fields, it is necessary to conduct field investigation in whole year and to evaluate P efflux from rice field during winter flooding.

To maximize the effect of winter flooding on P removal in irrigation water, fertilizer addition should be conducted at the same time as the first puddling operation, because when conducted several times, puddling operations may produce oxidizing conditions in soil. Puddling is also expected to increase the efficiency of a fertilizer because Fe bound or absorbed P is regarded as bioavailable in rice fields (Liu et al. 2016), though further research is required to characterize the factors that control redox conditions in soil during and following winter flooding and to conclude the mechanism of P reduction by winter flooding. To practice winter flooding in the context of environmental conservation in rice fields, it is necessary to evaluate the effects of winter flooding on yields and qualities of rice. Winter flooding can be easily implemented on clay soils and with available water resources. Thus, winter flooding is a valuable application that may conserve the agricultural environment and maintain water quality and biodiversity.

Acknowledgments

This research was supported by the RIHN Project (grant no. D06-14200119) and JSPS KAKENHI Grant Number JP19K15723. We thank to the Kosaji Environmental Conservation Committee for introducing sampling paddies and supporting the sampling. The experiments comply with the current laws of Japan.

References

Asano, S. Wakita K, Saizen I, Ishida T, Okuda N (2018) Advancement of biodiversity conservation activities with detecting local environmenal icons. J Rural Planning 37:150–156.

Carpenter SR, Caraco NF, Correll DL, Howarth RW, Sharpley AN, Smith VH (1998) Nonpoint pollution of surface waters with phosphorus and nitrogen. Ecol Appl 8:559–568. doi: 10.2307/2641247

Day PR (1965) Particle fractionation and particle-size analysis. In Method of Soil Analysis, Part 1. American Society of Agronomy, Madison, pp 547-567.

Dodds WK (2003) The role of periphyton in phosphorus retention in shallow freshwater aquatic systems. J Phycol 39:840–849. doi: 10.1046/j.1529-8817.2003.02081.x

Fitzgerald GJ, Scow KM, Hill JE (2000) Fallow season straw and water management effects on methane emissions in California rice. Global Biogeochem Cycles 14:767–776. doi: 10.1029/2000GB001259

Hua L, Liu J, Zhai L, Xi B, Zhang F, Wang H, Liu H, Chen A, Fu B (2017) Risks of phosphorus runoff losses from five chinese paddy soils under conventional management practices. Agriculture, Ecosystems and Environment 245:112–123. doi: 10.1016/j.agee.2017.05.015

Huang W, Cai W, Huang H, Lei Z, Zhang Z, Tay JH, Lee DJ (2015) Identification of inorganic and organic species of phosphorus and its bio-availability in nitrifying aerobic granular sludge. Water Res 68:423–431. doi: 10.1016/j.watres.2014.09.054

Hupfer M, Gächter R, Giovanoli R (1995) Transformation of phosphorus species in settling seston and during early sediment diagenesis. Aquat Sci 57:305–324. doi: 10.1007/BF00878395

Inubushi K, Wada H, Takai Y (1982) Variation of chlorophyll a concentration in paddy soil (in Japanese). Jpn Soc Soil Sci Plant Nutr 53:277–282. doi: 10.20710/dojo.53.4_277

Ishida T, Uehara Y, Iwata T, Cid-Andres AP, Asano S, Ikeya T, Osaka K, et al (2019) Identification of phosphorus sources in a watershed using a phosphate oxygen isoscape approach. Environ Sci Technol 53:4707–4716. doi:10.1021/acs.est.8b05837

JIS (1993) Testing Method for Industrial Wastewater, JIS K 0102. Japan Standard Association, Tokyo.

Kagatsume T. (2012) Water conservation policy of shiga prefectural government. In Hiroya Kawanabe, Machiko Nishino, and Masayoshi Maehata (ed) Lake Biwa: Interactions between Nature and People. Springer, Dordrecht, pp 423–427. doi:

10.1007/978-94-007-1783-1

Kim K, Kim B, Eum J, Seo B, Shope C, Peiffer S (2018) Impacts of land use change and summer monsoon on nutrients and sediment exports from an agricultural catchment. Water 10. doi: 10.3390/w10050544

Kögel-Knabner I, Amelung W, Cao Z, Fiedler S, Frenzel P, Jahn R, Kalbitz K, Kölbl A, Schloter M (2010) Biogeochemistry of paddy soils. Geoderma 157:1–14. doi: 10.1016/j.geoderma.2010.03.009

Kudo Y, Noborio K, Shimoozono N, Kurihara R, Minami H (2017) Greenhouse gases emission from paddy soil during the fallow season with and without winter flooding in central japan. Paddy and Water Environment 15:217–220. doi: 10.1007/s10333-016-0523-5

Li JY, Deng KY, Hesterberg D, Xia YQ, Wu CX, Xu RK (2017) Mechanisms of enhanced inorganic phosphorus accumulation by periphyton in paddy fields as affected by calcium and ferrous ions. Sci Total Environ 609:466–475. doi: 10.1016/j.scitotenv.2017.07.117

Liu, Junzhuo, Xiongxin Luo, Naiming Zhang, and Yonghong Wu. 2016. “Phosphorus released from sediment of Dianchi lake and its effect on growth of Microcystis aeruginosa. Environ Sci Pollut Res 23:16321–16328. doi: 10.1007/s11356-016-

6816-9

Makiyama M, Tsukamoto T (2006) The process of cooperation between winter-flooded rice field and no-tillege rice farming, and foresight of this culture. Journal of the Agricultural Engineering Society, Japan 74:719–722.

Mao Y, Yang S, Yue Q, Wang W (2016) Theoretical and experimental study of the mechanisms of phosphate removal in the system containing Fe(III)-ions. Environ Sci Pollut Res 23:24265–24276. doi: 10.1007/s11356-016-7672-3

Ministry of Internal Affairs and Communications (MIC) (2018) Statistical Handbook of Japan.

Murphy JA, Riley JP (1962) A modified single solution method for the determination of phosphate in natural waters. Analytica Chimica Acta 27:31–36. doi: 10.1016/S0003-2670(00)88444-5

Okubo T, Sato Y, Azuma Y (2014) Pollution loadings of paddy fields during irrigation period including runoff by rain events (in Japanese). Journal of Japan Society on Water Environment 37:229–237

R Core Team (2018) R: A language and environment for statistical computing. R foundation for statistical computing. Vienna, Austria. https://www.r-project.org/

Reddy KR, Kadlec RH, Flaig E, Gale PM (1999) Phosphorus retention in streams and wetlands: a review. Crit Rev Environ Sci Technol 29:83–146. doi: 10.1080/10643389991259182

Reynolds CS, Davies PS (2001) Sources and bioavailability of phosphorus fractions in freshwaters: a British perspective. Biol Rev Camb Philos Soc 76:27–64. doi: 10.1111/j.1469-185X.2000.tb00058.x

Scinto LJ, Reddy KR (2003) Biotic and abiotic uptake of phosphorus by periphyton in a subtropical freshwater wetland. Aquat Bot 77:203–222. doi: 10.1016/S0304-3770(03)00106-2

Sharpley AN, Herron S, Daniel T (2007) Overcoming the challenges of phosphorus-based management in poultry farming. J Soil Water Conserv 62:375–389.

Sharpley A (2016) Managing Agricultural phosphorus to minimize water quality impacts. Scientia Agricola 73:1–8. https://doi.org/10.1590/0103-9016-2015-0107.

Somura H, Masunaga T, Mori Y, Takeda I, Ide JI, Sato H (2015) Estimation of nutrient input by a migratory bird, the Tundra swan (Cygnus columbianus), to winter-flooded paddy fields. Agriculture, Ecosystems and Environment 199:1–9. doi: 10.1016/j.agee.2014.07.018

Soil Survey Staff (2010) Keys to soil taxonomy. Department of Agriculture: Natural Resources Conservation Service.

Suzuki R, Ishimaru T (1990) An improved method for the determination of phytoplankton chlorophyll using n, n-dimethylformamide. J Oceanogr 46:190–194. doi: 10.1007/BF02125580

Takada MB, Takagi S, Iwabuchi S, Mineta T, Washitani I (2014) Comparison of generalist predators in winter-flooded and conventionally managed rice paddies and identification of their limiting factors. SpringerPlus 3:418. doi: 10.1186/2193-1801-3-418

Takamura Y, Tabuchi Y, Suzuki S, Harigae Y, Ueno T, Kubota H (1976) The fates and balance sheets of fertilizer nitrogen and phosphorus applied to a rice paddy field in the Kasumigaura basin (in Japanese). Japanese Society of Soil Science and Plant Nutrition 47:398–405. doi: 10.20710/dojo.47.9_398

Tarapchak SJ, Rubitschun C (1981) Comparisons of soluble reactive phosphorus and orthophosphorus concentrations at an offshore station in Southern Lake Michigan. J Great Lakes Res 7:290–298. doi: 10.1016/S0380-1330(81)72057-4

Udo A, Jiku F, Okubo T, Nakamura M (2000) Mass Balances of water and nutrients in a paddy field (in Japanese). Journal of Japan Society on Water Environment 23:298–304. doi: 10.2965/jswe.23.298

Woodruff SL, House WA, Callow ME, Leadbeater BS (1999) The effects of biofilms on chemical processes in surficial sediments. Freshw Biol 41:73–89. doi: 10.1046/j.1365-2427.1999.00387.x

Yamada Y, Igeta A, Nakashima S, Mito Y, Ogasahara T, Wada S, Ohno T, Ueda A, Hyodo F, Imada M, Yachi S (2006) The runoff of suspended, substances, nitrogen, and phosphorus by enforced draining during the ploughing season experiments in paddy fields. Jpn J Limnol 67:105–112. doi: 10.3739/rikusui.67.105

Yi R, Song P, Liu X, Maruo M, Ban S (2019) Differences in dissolved phosphate in shallow-lake waters as determined by spectrophotometry and ion chromatography. Limnology. doi: 10.1007/s10201-019-00574-2

Zhou W, Lin S, Wu L, Zhao J, Wang M, Zhu B, Mo Y, Hu R, Chadwick D, Shaaban M (2017) Substantial N_2O emission during the initial period of the wheat season due to the conversion of winter-flooded paddy to rice-wheat rotation. Atmos Environ 170:269–278. doi: 10.1016/j.atmosenv.2017.09.021

Table and Figure Captions

Table 1. Soil pH, organic matter content, soil texture and phosphorous (P) concentrations of each fraction in initial soil samples. Flooding date indicates the start date of winter flooding.

Table 2. The guaranteed nutrient concentrations in chemical and organic fertilizers used for the incubation experiment and theoretical initial TP concentration after adding the fertilizers calculated by fertilizer amounts and concentrations and water volume in the incubation tubes.

Table 3. Model fits for log-transformed TP in incubation water in every sampling site, with only full and the best models. *(Day | incubation tube ID) indicates that tube ID was designated as a random-group factor and numerical day-after incubation as a random slope.

**Model fit was evaluated by AIC, assuming the model Degree of Freedom (DF) as shown in the table.

Fig. 1. Maps of the study area and sampling sites

Fig. 2. Initial phosphorous (P) concentrations of each fraction in incubated water; error bars indicate standard errors of the mean (S.E.). WF, winter flooding; CT, control no winter flooding; NRP, nonreactive phosphorous; SRP, soluble reactive phosphorous; PP,

particle phosphorous

Fig. 3. Average TP concentrations in incubated water from all sites and from sites K4 and K5; error bars indicate S.E.

Fig. 4. Average SRP concentrations in incubated water from all sites, and from sites K4 and K5; error bars indicate S.E.

Fig. 5. Oxidation–reduction potentials (ORP) in surface soils from all sites and from sites K4 and K5; error bars indicate S.E.

Fig. 6. Average chl *a* concentrations in surface soil samples from all sites and from sites K4 and K5; error bars indicate S.E.

Figure

Fig. 1. Maps of the study area and sampling sites

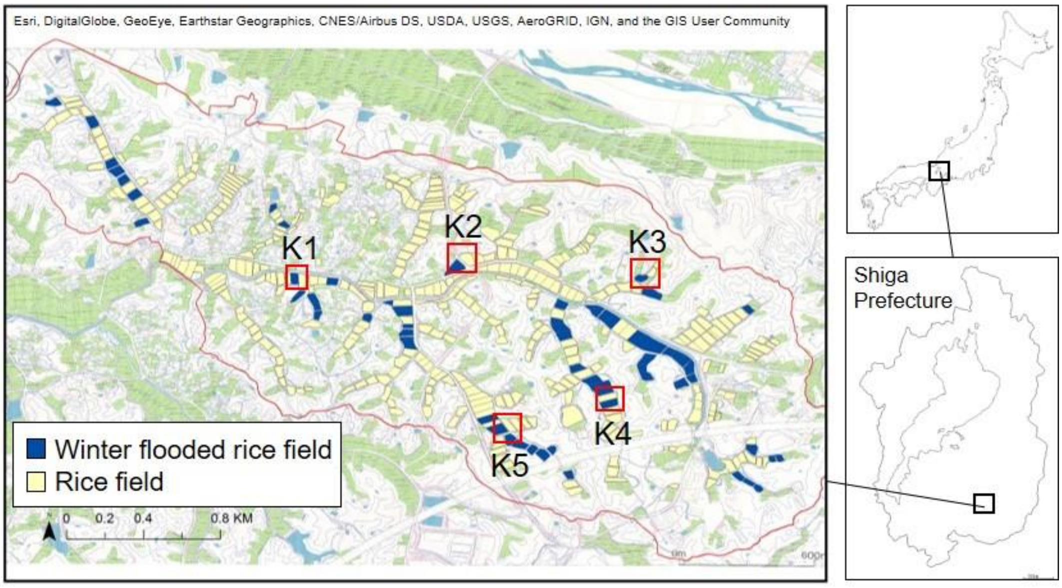

Fig. 2. Initial phosphorous (P) concentrations of each fraction in incubated water; error bars indicate standard errors of the mean (S.E.). WF, winter flooding; CT, control no winter flooding; NRP, nonreactive phosphorous; SRP, soluble reactive phosphorous; PP, particle phosphorous

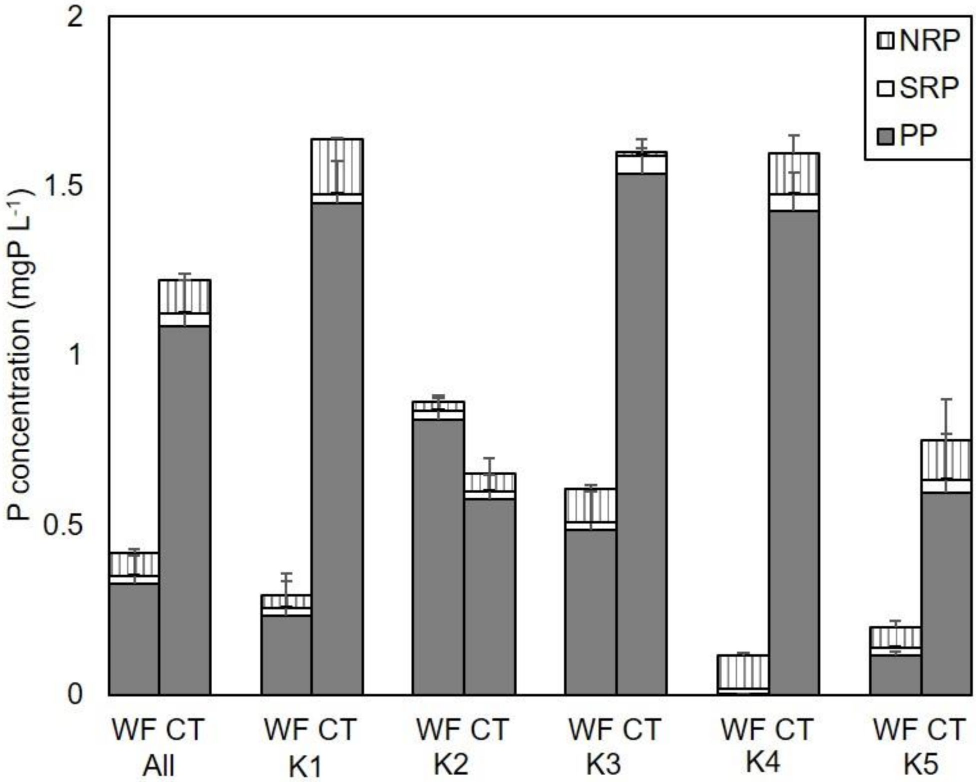

Fig. 3. Average TP concentrations in incubated water from all sites and from sites K4 and K5; error bars indicate S.E.

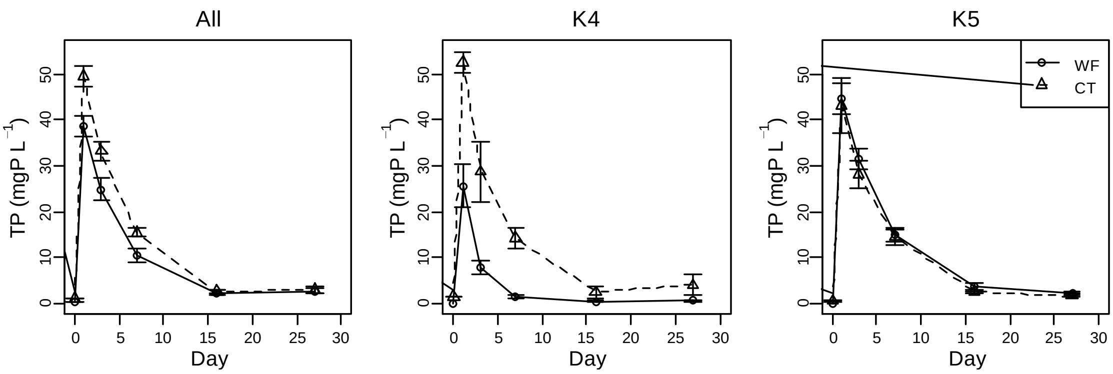

Fig. 4. Average SRP concentrations in incubated water from all sites, and from sites K4 and K5; error bars indicate S.E.

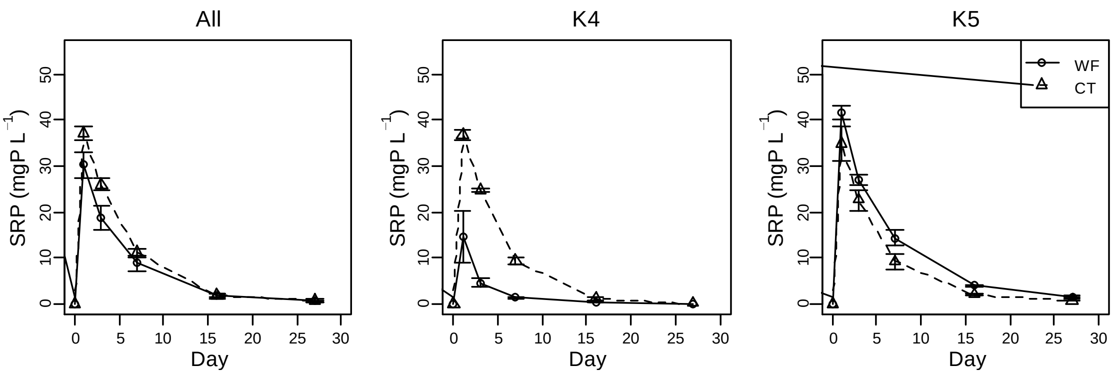

Fig. 5. Oxidation–reduction potentials (ORP) in surface soils from all sites and from sites K4 and K5; error bars indicate S.E.

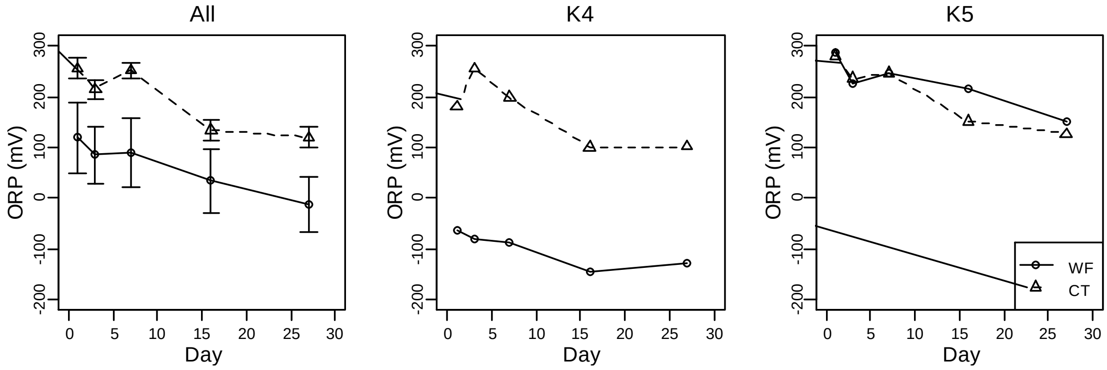

Fig. 6. Average chl *a* concentrations in surface soil samples from all sites and from sites K4 and K5; error bars indicate S.E.

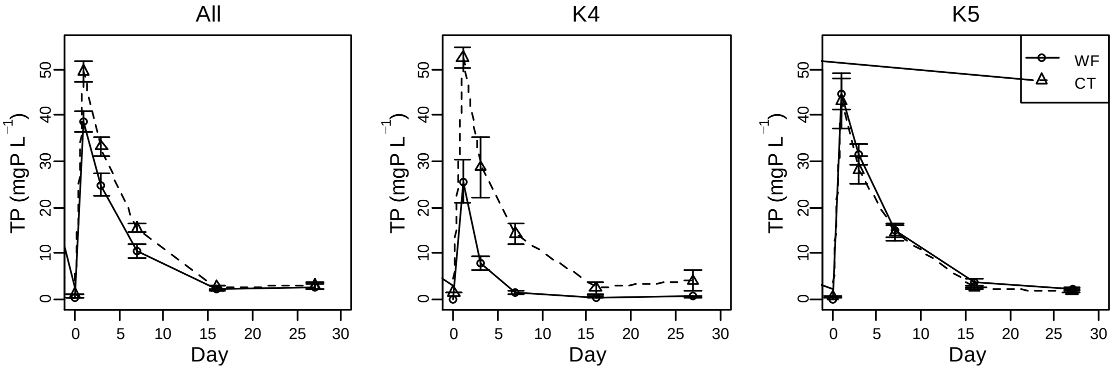

Table

Table 1. Soil pH, organic matter content, soil texture and phosphorous (P) concentrations of each fraction in initial soil samples. Flooding date indicates the start date of winter flooding.

Site		K1		K2		K3		K4		K5	
Flooding practice		WF	CT	WF	CT	WF	CT	WF	CT	WF	CT
Flooding date		2017/1/20		2016/12/7		2017/2/2		2017/1/30		2016/12/7	
Soil pH		5.95	5.91	5.93	5.85	6.27	6.20	5.68	5.81	5.98	5.81
Organic matter (g kg^{-1})		145	101	98.1	106	56.9	93.0	84.3	93.5	101	120
Textural information (%)											
	Sand (1000-19 μm)	21	23	22	26	23	26	49	50	16	21
	Silt (19-1.9 μm)	57	56	57	56	54	53	37	37	61	58
	Clay (<2 μm)	22	21	21	18	23	21	14	13	23	21
P concentration (mgP kg^{-1})											
	NH_4Cl-SRP	0.11	0.12	0.14	0.17	0.07	0.19	0.27	0.31	0.17	0.37

NH4Cl-NRP	1.00	1.12	0.87	1.07	0.64	1.04	0.85	0.96	0.91	1.27
BD-SRP	93.8	72.3	105	95.6	90.3	92.2	121	132	35.1	67.2
BD-NRP	0.00	0.00	0.00	2.40	3.87	15.0	51.3	58.0	23.2	39.8
NaOH-SRP	257	240	226	262	230	276	409	434	390	479
NaOH-NRP	338	295	262	317	252	337	157	203	173	226
HCl-SRP	48.5	93.6	92.2	99.4	104	82.1	54.8	56.5	29.0	60.2
HCl-NRP	257	216	171	233	173	224	46.3	44.0	60.4	46.6
Sum	995	919	858	1010	855	1028	840	929	712	921

Table 2. The guaranteed nutrient concentrations in chemical and organic fertilizers used for the incubation experiment and theoretical initial TP concentration after adding the fertilizers calculated by fertilizer amounts and concentrations and water volume in the incubation tubes.

Fertilizer type		Chemical fertilizer	Organic fertilizer	Sum
Nutrient concentration (%)				
	P	9.1	2.0	
	N	-	9.0	
	Fe	2.0	-	
	K	-	6.0	
	Mg	6.0	-	
Theoretical initial concentration (mg L^{-1})				
	P	45.5	10.0	55.5
	N	-	45.0	45.0
	Fe	10.0	-	10.0
	K	-	30.0	30.0
	Mg	30.0	-	30.0

Table 3. Model fits for log-transformed TP in incubation water in every sampling site, with only full and the best models. *(Day | incubation tube ID) indicates that tube ID was designated as a random-group factor and numerical day-after incubation as a random slope. **Model fit was evaluated by AIC, assuming the model Degree of Freedom (DF) as shown in the table.

Site	Response variable	Fixed variable	Random structure*	model AIC**	null AIC	model DF
K1	***ln*(Water-TP) (Day 1 to 27)**	**Day + Water flooding practice**	**(Day | incubation tube ID)**	**105**	**113**	**7**
K1	*ln*(Water-TP) (Day 1 to 27)	Day x Water flooding practice	(Day | incubation tube ID)	111	113	8
K2	***ln*(Water-TP) (Day 1 to 27)**	**Day**	**(Day | incubation tube ID)**	**106**	**114**	**6**
K2	*ln*(Water-TP) (Day 1 to 27)	Day x Water flooding practice	(Day | incubation tube ID)	114	114	8
K3	***ln*(Water-TP) (Day 1 to 27)**	**Day**	**(Day | incubation tube ID)**	**22**	**31**	**6**
K3	*ln*(Water-TP) (Day 1 to 27)	Day x Water flooding practice	(Day | incubation tube ID)	27	31	8
K4	***ln*(Water-TP) (Day 1 to 27)**	**Day + Water flooding practice**	**(Day | incubation tube ID)**	**108**	**125**	**7**

K4	*ln*(Water-TP) (Day 1 to 27)	Day x Water flooding practice	(Day | incubation tube ID)	114	125	8
K5	***ln*(Water-TP) (Day 1 to 27)**	**Day**	**(Day | incubation tube ID)**	**54**	**70**	**6**
K5	*ln*(Water-TP) (Day 1 to 27)	Day x Water flooding practice	(Day | incubation tube ID)	66	70	8